

## BASIC RESEARCH

# Regional Differences in Viscosity, Elasticity, and Wall Buffering Function in Systemic Arteries: Pulse Wave Analysis of the Arterial Pressure-Diameter Relationship

Daniel Bia,<sup>a,b</sup> Ismael Aguirre,<sup>a</sup> Yanina Zócalo,<sup>a</sup> Lucía Devera,<sup>a</sup> Edmundo Cabrera Fischer,<sup>c,d</sup> and Ricardo Armentano<sup>a,c</sup>

<sup>a</sup>Departamento de Fisiología, Facultad de Medicina, Universidad de la República, Montevideo, Uruguay.

<sup>b</sup>Facultad de Enfermería, Universidad de la República, Montevideo, Uruguay.

<sup>c</sup>Universidad Favaloro, Buenos Aires, Argentina.

<sup>d</sup>Consejo Nacional de Investigaciones Científicas y Técnicas, Buenos Aires, Argentina.

**Introduction and objectives.** Regional variations in the incidence of vascular diseases have been related to regional differences in arterial viscoelasticity. The aim of this study was to characterize the differences in the elastic and viscous modulus and in wall buffering function between central and peripheral systemic arteries, through a time-series analysis of the pressure-diameter relationship.

**Material and method.** Pressure and diameter were measured in 7 arterial segments (carotid, brachiocephalic trunk, ascending aorta, proximal, middle, and distal descending thoracic aorta, and femoral artery) from 6 sheep. Each segment was mounted on an *in vitro* mock circulatory system and perfused with Tyrode solution, with a pulse frequency of 1.8 Hz and systemic pressure levels. We used the Kelvin-Voigt model to calculate the pressure-diameter elastic ( $E_{pd}$ , mmHg/mm) and viscous ( $V_{pd}$ , mm Hg·s/mm) modulus, and to quantify the local wall buffering function ( $V_{pd}/E_{pd}$ ). We also calculated the incremental Young's and pressure-strain elastic modulus and pulse wave velocity for each segment.

**Results.** The elastic and viscous modulus increased from proximal to distal segments. The wall buffering function did not differ significantly between arteries. The lower rigidity of the central arteries compared to the distal ones may indicate that the systolic arterial compliance function is concentrated in the central arterial segments. On the other hand, the greater viscosity in the distal segments may indicate that viscous energy loss is concentrated in these segments.

**Conclusions.** Arterial elasticity and viscosity can be interpreted as properties that are dependent on the region of the vessel, whereas wall buffering function can be considered region-independent.

**Key words:** Basic research. Viscoelasticity. Arterial wall.

SEE EDITORIAL ON PAGES 121-5

Correspondence: Dr. Daniel Bia.  
Departamento de Fisiología. Facultad de Medicina.  
General Flores 2125. 11800 Montevideo. Uruguay.  
E-mail: dbia@fmed.edu.uy

Received March 29, 2004.

Accepted for publication November 2, 2004.

## Diferencias regionales en viscosidad, elasticidad y amortiguamiento parietal de arterias sistémicas: análisis isopulsátil de la relación presión-diámetro arterial

**Introducción y objetivos.** Variaciones regionales en la incidencia de diversas afecciones vasculares se han relacionado con diferencias regionales en la viscoelasticidad arterial. El objetivo de este trabajo fue caracterizar las diferencias regionales en el módulo elástico, viscoso y en el amortiguamiento parietal de arterias sistémicas, centrales y periféricas, mediante el análisis de la relación instantánea presión-diámetro arterial en el dominio temporal.

**Material y método.** Se midieron la presión y el diámetro en 7 segmentos arteriales extraídos de 6 ovejas: carótida, tronco braquiocefálico, aorta ascendente, aorta torácica descendente proximal, media y distal, y arteria femoral. Cada segmento fue montado en un sistema circulatorio *in vitro* y perfundido con solución Tyrode, con frecuencia de estimulación de 1,8 Hz y valores de presión sistémica. Utilizando un modelo Kelvin-Voigt, se obtuvieron el módulo presión-diámetro elástico ( $E_{pd}$ , mmHg/mm) y viscoso ( $V_{pd}$ , mmHg·s/mm), y se cuantificó la función de amortiguamiento parietal (FAP) como  $V_{pd}/E_{pd}$ . Adicionalmente, se calculó el módulo de Young incremental y elástico presión-deformación y la velocidad de onda del pulso de cada segmento.

**Resultados.** Los módulos elásticos y viscoso aumentaron hacia los segmentos periféricos, mientras que la FAP no mostró diferencias entre segmentos. La menor rigidez en las arterias centrales y la mayor viscosidad en las arterias periféricas podrían indicar que la función de reservorio arterial sistólico se concentra en las primeras y la disipación viscosa de energía en las segundas.

**Conclusiones.** La respuesta elástica y viscosa arterial podrían considerarse dependientes de la región arterial, mientras que la constante de FAP sería un indicador independiente de la región arterial.

**Palabras clave:** Investigación básica. Viscoelasticidad. Pared arterial.

## ABBREVIATIONS

$E_{pd}$ : pressure-diameter elastic modulus.  
 $V_{pd}$ : pressure-diameter viscous modulus.  
 WBF: wall buffering function.  
 $E_p$ : pressure-strain elastic modulus.  
 EINC: incremental Young's modulus.

## INTRODUCTION

The viscoelastic properties of the great arteries determine their main functions: to conduct blood (conductive function) and to buffer the pulse pressure and flow generated by ventricular ejection (wall buffering function, WBF).<sup>1,2</sup> Various diseases that affect arterial viscoelasticity have a diffuse presentation with affected and healthy segments interspersed.<sup>3</sup> Consequently, “global” or “regional” indices of arterial function (eg, total compliance) are unable to detect early-stage vascular disorders.<sup>3,4</sup> In addition, the incidence, severity, and predominance of a given vascular condition (eg, arteriosclerosis) differs according to the location of the segment under consideration in the arterial tree.<sup>5</sup> This observation has been linked to differences in the viscoelastic properties of the different arteries.<sup>5</sup> The diffuse nature and regional differences in vascular conditions have led to an increasing interest in identifying biomechanical differences between systemic arteries and undertaking clinical evaluations of the “local” function of individual segments.<sup>5</sup> To this end, systems have begun to be used that allow the instantaneous arterial pressure-diameter relationship to be monitored.<sup>6,7</sup>

In general, the elastic and viscous properties of the arterial wall have been characterized together as “viscoelasticity.”<sup>8</sup> Various studies have demonstrated that the elasticity and viscosity of the arterial wall play different roles in arterial function,<sup>1,2</sup> and can also be independently affected by physiologic, pathologic or experimental conditions.<sup>1,2,6,7,9,10</sup> Consequently, adequate evaluation of local arterial function requires separate characterization of the elastic and viscous responses, and with them the WBF. In light of this, we have recently proposed the determination of WBF through the relationship between the arterial viscous and elastic moduli.<sup>1,2,9</sup>

In general, the viscous response has not been considered when evaluating arterial function. This is mainly due to methodological difficulties; the nonlinear character of the arterial pressure-diameter relationship is the principal limitation to the determination

of the response in the frequency domain.<sup>8,9,11</sup> To characterize it, we have used a series of procedures in the time domain that were originally proposed by Bauer.<sup>12</sup> Using these procedures, the nonlinear character of the pressure-diameter relationship does not present significant difficulties.<sup>1,2,13</sup>

The dependence of the elastic and viscous responses on mean and pulse pressures and stimulation frequency, among other factors, means that to compare the viscous and elastic moduli of different arterial segments, they must be analyzed under identical experimental conditions, including those of the normal work of each segment. Although it has been suggested that the arterial viscoelastic response displays regional differences,<sup>8,11</sup> to our knowledge there have been no studies in which such differences have been characterized using dynamic, isobaric analyses, which analyze the instantaneous pressure and diameter signals in the time domain and characterize viscosity and elasticity separately. Likewise, we are unaware of any study in which possible differences in the local WBF have been assessed.

The aim of this study was to characterize the regional differences in the elastic and viscous responses of the arterial wall, and in the WBF of the central and peripheral systemic arteries using dynamic and isobaric analysis of the arterial pressure-diameter relationship in the time domain. In addition, the intrinsic elastic response of the artery was quantified using parameters that allowed its rigidity to be characterized independently of the arterial dimension.

## MATERIALS AND METHODS

### Surgical Preparation

Six Merino sheep (35 kg to 45 kg) were anesthetized with intravenous sodium pentobarbital (35 mg/kg). The neurovascular bundle of the neck and right hind limb were dissected and bilateral thoracotomy was performed. Segments (5 cm long; marked by adventitious sutures) were dissected from the right carotid artery, the brachiocephalic trunk, the right femoral artery, the ascending thoracic aorta, and the proximal, medial, and distal descending thoracic aorta (Figure 1). A pressure microtransducer (Konigsberg Instruments Inc., Pasadena, USA), calibrated at 37°C using a mercury manometer, was introduced into each segment. A pair of ultrasound crystals (5 MHz, 2 mm diameter) were sutured to the adventitia in diametrically opposed sites and connected to a sonomicrometer (Triton Technology Inc., San Diego, USA). The transit time of the signal between the crystals (ultrasound velocity: 1580 m/s) allowed the instantaneous diameter of the segment to be calculated.<sup>1,2</sup> Following instrumentation, the selected arterial segments were excised with the sensors located in their medial por-

tion. Finally, the animals were sacrificed by pentobarbital overdose and intracardiac administration of potassium chloride. All procedures were performed in accordance with international guidelines.<sup>14</sup> The methods used had been employed previously by our group.<sup>1,2,9,13,15</sup>

### In Vitro Studies

The excised arterial segments were mounted in an in vitro perfusion system<sup>15</sup> (Figure 2) made up of polyethylene tubing, a tubular resistance regulator, a reservoir containing Tyrode's solution, and an artificial heart (Jarvik Model 5, Kolff Medical Inc., Salt Lake City, USA) fed by a pneumatic electric pump.<sup>15</sup> The arterial segments were mounted in a gap in the tubing and the ends were attached to the tubes using ligatures, thereby closing the system and allowing circulation of oxygenated Tyrode's solution at 37°C, pH 7.40. The arterial segments were studied at the same length as in vivo. Thus, when they were mounted in vitro, they were extended; the average extension ratio ( $\lambda$  = length in vivo/excised length) was 1.25. The mounted segment was immersed in Tyrode's solution. The pulse-pressure range and pumping frequency were regulated by the pump controls, while altering the resistance and reservoir height allowed the mean pressure and the form of the pressure waves to be controlled. After mounting the segment, it was left for 10 minutes under conditions of stable pressure, flow, and pumping frequency prior to beginning measurements. During this period, the diameter signal was calibrated in millimeters using the calibration system of the sonomicrometer.<sup>1,2,9,13</sup>

### Experimental Protocol

The diameter and pressure of each segment was determined and stored during a single stable period. The pumping frequency was similar to the cardiac frequency of the sheep.<sup>1,2</sup> The segments were subjected to pressure pulses that were similar in shape and magnitude to those observed for the systemic circuit under physiological conditions (Figure 3). At the end of the experiment, the segments were weighed.

### Data Collection and Analysis

The diameter and pressure signals were visualized in real time and digitized (sampling frequency of 200 Hz). For each segment, 20 to 30 consecutive beats were stored.

#### Quantification of the Elastic and Viscous Response

Representation of the arterial wall through a Kelvin-

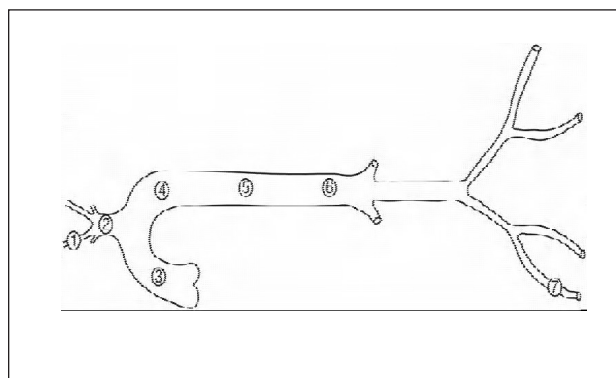


**Figure 1.** Arterial segments studied. 1 indicates the carotid artery; 2, the brachiocephalic trunk; 3, the ascending aorta; 4, the proximal descending thoracic aorta; 5, the medial descending thoracic aorta; 6, the distal descending thoracic aorta, and 7, the femoral artery.

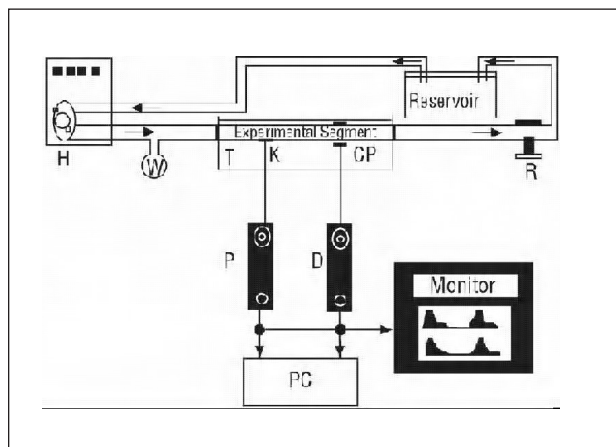


**Figure 2.** In vitro system. H indicates pneumatic pump and artificial heart; K, pressure sensor (Konigsberg); GP, diameter sensor (ceramic piezoelectric); P, pressure signal; D, diameter signal, and PC, computer. Arrows indicate the direction of flow. T, container filled with Tyrode's solution. Reservoir contains Tyrode's solution. W indicates a distensible chamber. R indicates a flow resistor.

Voigt viscoelastic model allowed the pressure-diameter elastic modulus ( $E_{pd}$ ) and the pressure-diameter viscous modulus ( $V_{pd}$ ) to be calculated.<sup>1,2,9</sup> The model considers the pressure exerted on the wall to be distributed in terms of an element representative of the wall elasticity (spring) and another that is representative of the wall viscosity (buffer).<sup>1,2,16</sup> The total observed pressure can be separated into elastic and viscous components:

$$P_{total} = P_{elastic} + P_{viscous} \quad [1]$$

Reordering equation [1] we obtain

$$P_{elastic} = P_{total} - P_{viscous} \quad [2]$$

The  $P_{viscous}$  is proportional to the first derivative of

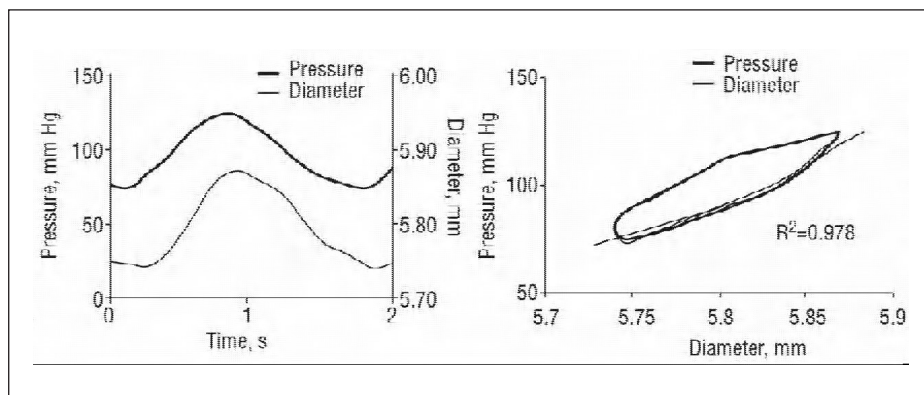


**Figure 3.** Left: femoral pressure and diameter signals. Right: femoral pressure-diameter relationship. Black lines indicate the total pressure-diameter relationship. Gray lines indicate the pure elastic pressure-diameter relationship, obtained after minimizing the area of hysteresis for calculation of the viscous modulus. Note the exponential adjustment to the pure elastic relation.

the diameter with respect to time<sup>1,2,9,13</sup>:

$$P_{elastic} = P_{total} - V_{pd} \frac{dD}{dt} \quad [3]$$

where  $V_{pd}$  is the wall viscous modulus and  $dD/dt$  is the first derivative of the diameter with respect to time. An arterial pressure-diameter relation was constructed from the temporal signals of pressure and diameter for each pulse to be analyzed.<sup>1,2</sup> For each pulse, the area of hysteresis of the pressure-diameter relation was reduced via an incremental-iterative computational procedure for the value of  $V_{pd}$  in equation [3].<sup>1,2</sup> Once the minimum area was obtained, the incremental-iterative procedure was stopped and the value of  $V_{pd}$  was considered equivalent to the viscous modulus.<sup>1,2</sup> Then, an exponential function was adjusted to the resulting pure elastic pressure-diameter relation, obtained upon elimination of the area of hysteresis (Figure 3)<sup>1,2</sup>:

$$P = \alpha \times e^{\beta \times D} \quad [4]$$

The  $E_{pd}$  was calculated as the slope of the function at the mean diastolic pressure<sup>1,2</sup>:

$$E_{pd} = \frac{dD}{dt} \text{ mean pressure} \quad [5]$$

### Wall Buffering Function

Using a Kelvin-Voigt model, the capacity of the arterial wall to buffer a pressure stimulus emerges from the relationship between the pressure stimulus and the resulting strain.<sup>1,2</sup> As in previous studies,<sup>1,2</sup> the WBF was quantified as

$$WBF = V_{pd} / E_{pd} \quad [6]$$

The lower the WBF, the lower the buffering capacity of the arterial wall.<sup>1,2</sup>

### Quantification of the Elastic Response: Parameters Independent of the Diameter

In order to compare the results obtained for elastic response with those from the literature, and to assess the regional differences in arterial rigidity independent of arterial dimensions, we calculated the incremental Young's modulus ( $E_{INC}$ ) and the clinical indicators pulse wave velocity and the pressure-strain elastic modulus ( $E_p$ ).

To calculate the  $E_{INC}$ , the arterial stress-strain relationship was constructed for each pulse to be analyzed.<sup>13,16</sup> Using a similar procedure to that described earlier, the area of hysteresis was eliminated and a pure elastic stress-strain relation was obtained.<sup>13</sup> The  $E_{INC}$  was then calculated as

$$E_{INC} = \frac{d\sigma}{d\varepsilon} \text{ mean stress} \quad [7]$$

where  $d\sigma$  and  $d\varepsilon$  are the first derivatives with respect to time of the circumferential stress and the arterial strain in the pure elastic relation, respectively.<sup>16</sup> The  $E_{INC}$  is always calculated for the  $d\sigma/d\varepsilon$  corresponding to the mean diastolic stress. The following equation was used to calculate  $\sigma$ <sup>13</sup>:

$$\sigma = 2P \frac{(R_i \times R_e)^2}{R_e^2 - R_i^2} \times \frac{1}{R^2} \quad [8]$$

where  $P$  is pressure,  $R_i$  is the internal arterial radius,  $R_e$  is the external arterial radius, and  $R$  is the mean arterial radius ( $R = [R_i + R_e] / 2$ ).<sup>13</sup> The strain ( $\varepsilon$ ) was calculated<sup>13</sup> as

$$\varepsilon = R / R_0 \quad [9]$$

where  $R_0$  is the arterial radius at a pressure of 0 mm Hg. The pulse wave velocity was calculated<sup>16</sup> as

TABLE 1. Hemodynamic Variables\*

	MP, mm Hg	PP, mm Hg	MD, mm
Carotid	98±4	67±11	7.92±1.61
Brachiocephalic trunk	95±5	68±10	19.93±0.68 <sup>a</sup>
Ascending aorta	97±6	67±13	22.73±2.40 <sup>a,b</sup>
Proximal descending aorta	97±5	72±15	19.67±0.98 <sup>a,c</sup>
Medial descending aorta	97±4	71±14	19.77±0.85 <sup>a,c</sup>
Distal descending aorta	95±6	72±12	17.57±1.72 <sup>a,e</sup>
Femoral	96±3	71±15	5.73±0.23 <sup>a-f</sup>

\*Values are expressed as mean H±DS. Letters <sup>a, b, c, d, e, f</sup> shown in superscript indicate *P*<.05 with respect to segments of the carotid artery, brachiocephalic trunk, ascending aorta, and proximal, medial, and distal descending aorta, respectively. MD indicates mean diameter; MP, mean pressure; and PP, pulse pressure..

$$PWV = \sqrt{\frac{E_{INC} \times h_m}{2 \times R_i \times \rho_s}} \quad [10]$$

where  $h_m$  is the mean wall thickness<sup>13</sup> and  $\rho_s$  is the blood density ( $\rho_s=1.06$  g/mL). The  $E_p$  was calculated<sup>16</sup> as

$$E_p = 1334 \times D_D \frac{P_S - P_D}{(D_S - D_D)} \quad [11]$$

where  $P_S$  and  $P_D$  are systolic pressure and diastolic pressure, respectively, and  $D_S$  and  $D_D$  are systolic diameter and diastolic diameter, respectively.

**Statistics**

For each arterial segment, the values of the hemodynamic and biomechanical parameters represent the mean of 20-30 beats. The values calculated for each artery type are expressed as the mean (SD). The presence of significant differences between the groups was assessed by ANOVA followed by the Bonferroni test. Statistical significance was set at *P*<.05.

**RESULTS**

Table 1 shows the hemodynamic stimulation variables and the mean diameter of each segment. Note that the segments were stimulated with similar pressure levels (isobaric studies), stimulation frequency (isofrequency studies), and using pressure waves similar to those encountered under physiological conditions (Figure 3). The use of isobaric comparisons ensured that differences observed in rigidity were not due to differences in the distension pressure. The use of isofrequency comparisons ensured that the differences seen between  $V_{pd}$  values were not due to differences in the wall stimulation velocity. Finally, note that the mean diameter decreased as the arteries became more peripheral.

Table 2 shows the mean values for the  $E_{pd}$  and  $V_{pd}$

TABLE 2. Viscoelastic Moduli and Wall Buffering Function\*

	$E_{pd}$ , mm Hg/mm	$V_{pd}$ , mm Hg x s/mm	WBF, $10^{-2}$ s
Carotid	1245±281	23.9±5.1	2.0±0.1
Brachiocephalic trunk	23±5 <sup>a</sup>	0.5±0.1 <sup>a</sup>	2.1±0.4
Ascending aorta	16±7 <sup>a,b</sup>	0.3±0.2 <sup>a,b</sup>	2.3±0.6
Proximal descending aorta	27±3 <sup>a,c</sup>	0.6±0.2 <sup>a,d</sup>	2.3±0.6
Medial descending aorta	28±3 <sup>a,c</sup>	0.6±0.2 <sup>a,c</sup>	2.5±0.6
Distal descending aorta	79±34 <sup>a-e</sup>	1.9±0.7 <sup>a-e</sup>	2.4±0.5
Femoral	355±110 <sup>a-f</sup>	6.8±2.2 <sup>a-f</sup>	2.0±0.3

\*Values are expressed as mean H±DS. Letters <sup>a, b, c, d, e, f</sup> shown in superscript indicate *P*<.05 with respect to segments of the carotid artery, brachiocephalic trunk, ascending aorta, and proximal, medial, and distal descending aorta, respectively.  $E_{pd}$  indicates the pressure-diameter elastic modulus; WBF, the wall buffering function; and  $V_{pd}$  the pressure-diameter viscous modulus.

TABLE 3. Pulse Wave Velocity, Pressure-Strain Elastic Modulus, and Incremental Young's Modulus\*

	PWV, m/s	$E_p$ , 105 dyn/cm <sup>2</sup>	EINC, 106 dyn/cm <sup>2</sup>
Carotid	23.2±1.1	135.0±28.3	101.0±36.4
Brachiocephalic trunk	4.9±0.3 <sup>a</sup>	8.2±1.0 <sup>a</sup>	5.6±1.0 <sup>a</sup>
Ascending aorta	4.7±0.9 <sup>a</sup>	6.5±1.4 <sup>a,b</sup>	4.4±0.9 <sup>a,b</sup>
Proximal descending aorta	5.4±0.2 <sup>a,c</sup>	8.1±1.6 <sup>a,c</sup>	5.2±0.7 <sup>a,c</sup>
Medial descending aorta	5.6±0.3 <sup>a,c</sup>	8.6±1.9 <sup>a,c</sup>	5.4±0.8 <sup>a,c</sup>
Distal descending aorta	8.6±1.2 <sup>a-e</sup>	20.9±7.4 <sup>a-e</sup>	23.4±6.9 <sup>a-e</sup>
Femoral	11.1±2.3 <sup>a-f</sup>	33.3±7.7 <sup>a-f</sup>	28.1±7.9 <sup>a-f</sup>

\*Values are expressed as mean±SD. Letters <sup>a, b, c, d, e, f</sup> shown in superscript indicate *P*<.05 with respect to segments of the carotid artery, brachiocephalic trunk, ascending aorta, and proximal, medial, and distal descending aorta, respectively. EINC indicates incremental Young's modulus;  $E_p$ , the pressure-strain elastic modulus; PWC, the pulse wave velocity

moduli and the WBF for each group of segments. Note that the  $E_{pd}$  and  $V_{pd}$  were higher the more peripheral the segment. This indicates that the arterial rigidity and the viscous response of the wall increase towards the periphery. Note also the slight increase in the  $E_{pd}$  and the  $V_{pd}$  between the ascending aortic and the proximal and medial descending aortic segments, and the sharp increase in the distal descending aortic, carotid, and femoral segments. In addition, observe that, despite the variation in the  $E_{pd}$  and  $V_{pd}$  between the different segments, the WBF did not show significant differences.

Table 3 shows the pulse wave velocity, the  $E_{INC}$ , and the  $E_p$ . The values obtained for these parameters are consistent with those seen in the literature.<sup>16</sup> Note that the pulse wave velocity and both elastic moduli increase towards the periphery. However, when using these parameters, which take into account the arterial geometry, the differences in the elastic response of the segments were lower than those found when using the  $E_{pd}$  modulus (Table 2).

The reduction did not alter the tendency of the elastic response to increase towards the periphery. However, it did mean that the differences in the  $E_{INC}$  and  $E_p$  seen between the brachiocephalic trunk and medial descending aorta were no longer statistically significant.

## DISCUSSION

The following discussion is focused on the 2 main findings from the study: *a*) the elastic and viscous response of the arteries, obtained from a time-series analysis of the arterial pressure-diameter relationship, increased towards the periphery, and *b*) despite the variation in the elastic and viscous response, the WBF did not show significant differences between segments.

### Elastic and Viscous Response: Regional Differences

Three moduli of elasticity previously defined and used by other authors<sup>1,2,7,16</sup> were used to evaluate the elastic response. This allowed comparison of the results obtained here with those found in the literature, as well as serving as a reference for future approaches. Although all of the moduli evaluate arterial rigidity, the different ways in which the calculations are performed generate complementary information relating to the mechanical properties of the arteries.<sup>16</sup> The  $E_{INC}$  is commonly used in elasticity theory because it best defines the intrinsic properties (independently of the geometry or size) of a given material (eg, the arterial wall).<sup>4,16</sup> Consequently, it is considered the “gold standard” for the evaluation of the elastic response of a material.<sup>16</sup> The requirement for the geometric characteristics of the arterial segment (thickness and diameter of the arterial wall) to be known makes this a difficult modulus to calculate in a clinical setting.<sup>14,16</sup> Due to the nonlinearity of the pure elastic stress-strain relation, calculation of the  $E_{INC}$  requires that the stress or strain for which it is calculated is systematized and determined. The calculated  $E_{pd}$  modulus can be measured in the clinic based on the signals for the instantaneous arterial pressure and diameter. Like the  $E_{INC}$ , the pressure or diameter for which it is calculated must be defined. It allows the arterial rigidity to be evaluated independently of the viscous properties of the arterial wall since it is calculated by eliminating the hysteresis of the pressure-diameter relation. Furthermore, it allows the WBF to be calculated, since it has units that are consistent with the  $V_{pd}$ . Finally, the  $E_p$  allows calculation of the arterial rigidity in relation to the unit strain, and as such, is independent of the diameter.<sup>16</sup> Its particular clinical usefulness comes from the fact that it is only necessary to know the maximum systolic and

minimum diastolic values of the arterial pressure and diameter signals in order to perform the calculation.<sup>16</sup> However, since the calculation requires the use of the maximum and minimum values for pressure and diameter in order to calculate the secant between these points, its value includes both the elastic and viscous behavior of the arterial wall. Thus, due to the viscoelastic characteristic of the arterial wall, the maximum systolic diameter of the artery reached during arterial distension is highly dependent upon the level of arterial viscosity.

The elastic response of the artery is an important determinant of its conductive and buffering roles.<sup>1,2,9,17-19</sup> An adequate elastic modulus allows systolic distension of the artery and the subsequent diastolic elastic recoil, which ensures the continuity of antegrade blood flow. In addition, an adequate elastic modulus reduces the oscillations generated by the heart,<sup>19</sup> minimizing the arterial and ventricular systolic pressure and increasing the arterial diastolic pressure, while ensuring that the mean arterial pressure is high and the pulsatility low.<sup>1,2</sup>

The relative importance of the elastic response of a segment over the heart, the arteries, and the microcirculation varies according to the site occupied by the segment in the vascular tree. Our data show that the ascending aorta presents the lowest elastic modulus (Tables 2 and 3). This could be related to the fact that it is the only segment that receives the entire ejected volume from the left ventricle, necessitating maximal distension capacity to minimize ventricular afterload. The elastic response tends to increase in more distal segments. However, no significant differences were seen between successive arterial segments from more proximal regions. This gradual increase in the elastic response in the thorax may indicate that these segments contribute to reducing the ventricular afterload and ensuring an adequate systolic arterial reservoir function.

Beyond the distal descending aortic segment, the elastic response of the arterial wall increases sharply, an observation that is in agreement with findings in canine arteries.<sup>16</sup> The degree of increase depends on the modulus used to characterize the elastic response. When using pulse wave velocity,  $E_{INC}$ , and  $E_p$ , the differences in elastic response between the peripheral segments, and between these and the central segments are lower than those obtained using the  $E_{pd}$ . However, the differences between peripheral and central segments continue to be high, demonstrating that they respond mainly to differences in arterial wall structure. The higher elastic modulus of the peripheral segments may be related to an increase in the fraction of collagen in the arterial wall and to the arterial “radius/thickness” ratio towards the periphery. Under isobaric conditions, the higher radius/thickness ratio would lead to a higher wall tension (Laplace law) in

the peripheral arteries,<sup>13</sup> compensated by a higher degree of wall rigidity, thereby preventing wall rupture.<sup>10,20</sup> In addition, it may indicate that their level of elastic response may be of relatively lesser importance than those of the central arteries for the determination of ventricular afterload.

The viscous response of the arterial wall causes the arterial system in systole to dissipate like heat, part of the energy imparted by the heart in each beat.<sup>1,2,13</sup> The viscosity attenuates the highest frequency components of the incident waves of pressure and flow<sup>19</sup> and the amplitude of the reflected waves that could trigger resonance phenomena in the system.<sup>17</sup> Furthermore, mechanical damage to the arterial wall would be reduced by eliminating the high frequencies that would cause early fatigue.<sup>9,19</sup> Thus, the viscosity contributes to the WBF.<sup>1,2,19</sup> In contrast to these beneficial functions, Milnor<sup>21</sup> postulated a damaging effect of viscosity caused by a 10% to 20% increase in ventricular afterload.

Our results show that wall viscosity, quantified using the  $V_{pd}$ , increases towards the periphery. The lower  $V_{pd}$  of the central arteries, which receive the ventricular ejection directly, could be considered as a “strategy” to minimize ventricular afterload. Given that the viscosity has been correlated with the net amount of smooth muscle cells in the arterial wall,<sup>1,9</sup> the higher  $V_{pd}$  of the peripheral arteries, and of the carotid compared with the femoral artery could be explained by higher levels of smooth muscle cells in the peripheral arteries,<sup>11,13</sup> and in the carotid with respect to the femoral artery.<sup>11</sup> The higher  $V_{pd}$  of the peripheral vessels would lead them to be the most responsible for energy dissipation from the vascular system.

### Wall Buffering: Regional Differences

Recently, in anesthetized animals, we found that the local WBF of the ascending aorta and the main pulmonary aorta is similar, despite their differences in elastic and viscous response.<sup>1</sup> In both arteries, under conditions of acute hypertension with activation of vascular smooth muscle cells, the WBF remained similar to the basal value, despite the increased pressure dependent upon the  $E_{pd}$ . This maintenance of the WBF is due to the increase in the  $V_{pd}$  modulus generated by the muscle activation. Based on these findings, we postulated that the WBF could be considered as an arterial constant that is independent of the hemodynamic circuit, and that mechanisms would exist in each circuit to maintain its high value irrespective of changes in the hemodynamic conditions.<sup>1</sup> In an effort to generate a better mechanical-functional characterization of the arteries, we sought to determine whether the WBF is a constant independent of the position in the systemic arterial circuit.

Our results do not show significant differences in

the WBF of the different segments studied. Consequently, they offer complementary information to that provided by earlier studies,<sup>1,2,9</sup> showing that, independently of the segment studied, the arterial wall displays a similar buffering capacity. This is in agreement with the results of Langewouters et al,<sup>22</sup> who, using a complex arterial model, found that the time constant for the arterial wall was similar in segments of the human thoracic and abdominal aorta in vitro. It can, therefore, be postulated that while the viscous and elastic responses are “fixed” according to the “position” of the segment under consideration, to ensure an adequate WBF, the relationship between the two responses is constant. Thus, in segments with the highest rigidity and, therefore, lower systolic reservoir capacity for potential energy, there is a higher capacity to dissipate energy, or higher viscosity, thereby ensuring an adequate WBF.

### Clinical Implications

Previous studies have demonstrated that the viscoelastic properties of the arteries vary in different physiological stages (eg, development)<sup>10</sup> and physiopathological states (eg, arteriosclerosis).<sup>7</sup> This study shows that, as for the elastic modulus, while the viscous modulus of a particular segment depends upon its position within the vascular tree, the relationship between them, an indicator of the WBF, remains constant. Changes in the moduli may indicate disease or an adaptive response of the arterial wall to a physiological or pathological state. Therefore, adequate local evaluation of the arteries requires determination of the viscous and elastic responses, of the WBF, and analysis of these parameters according to status of the patient. In addition, given the resemblance of the viscoelastic response between the native artery and the substitute artery used in vascular reconstruction (eg, arterial bypass) is correlated with a lower rate of prosthetic failure,<sup>23</sup> knowledge of the mechanical properties of a given arterial segment is fundamental for the selection of a substitute artery.

The study methods and analysis used would allow to simply assess the extent to which different vascular segments are compromised in different disease states, their response to treatment, and their adaptation to different physiological or pathological situations. Thus, systems have recently begun to be used for the local evaluation of arterial function (eg, intravascular ultrasound, echography, and applanation tonometry) that allow continuous in vivo monitoring of the diameter and pressure signal of the arterial “ring” of interest.<sup>4,6,7</sup> In the future, based on these signals and using the methods described here, it will be possible to characterize the mechanical-functional properties presented, with the described clinical implications.

## CONCLUSIONS

The viscous and elastic response and the WBF were characterized separately using a simple viscoelastic model (Kelvin-Voigt) and methods for the analysis of the instantaneous pressure and diameter in the time domain. Regional differences in these variables were then analyzed. In addition, differences in the pulse wave velocity, the  $E_{INC}$ , and the  $E_p$  were characterized for the different segments studied. The elastic and viscous moduli increased towards the periphery, showing them to be dependent upon the arterial region. In contrast, the WBF remained constant, independently of the segment analyzed, and was considered to be a property that is independent of the arterial region.

## ACKNOWLEDGMENT

To Mr Elbio Agote for technical assistance.

## REFERENCES

- Bia D, Armentano RL, Grignola JC, Craiem D, Zócalo YA, Ginés FF, et al. El músculo liso vascular de las grandes arterias: ¿sitio de control local de la función de amortiguamiento arterial? *Rev Esp Cardiol*. 2003;56:1202-9.
- Bia D, Armentano R, Craiem D, Grignola J, Ginés F, Simon A, et al. Smooth muscle role on pulmonary arterial function during acute pulmonary hypertension in sheep. *Acta Physiol Scand*. 2004;181:359-66.
- Chandran KB, Mun JH, Choi KK, Chen JS, Hamilton A, Nagaraj A, et al. A method for in-vivo analysis for regional arterial wall material property alterations with atherosclerosis: preliminary results. *Med Eng Phys*. 2003;25:289-98.
- McVeigh GE, Hamilton PK, Morgan DR. Evaluation of mechanical arterial properties: clinical, experimental and therapeutic aspects. *Clinical Science*. 2002;102:51-67.
- Länne T, Hansen F, Mangell P, Sonesson B. Differences in mechanical properties of the common carotid artery and abdominal aorta in healthy males. *J Vasc Surg*. 1994;20:218-25.
- Stefanadis C, Stratos C, Vlachopoulos C, Marakas S, Boudoulas H, Kallikazaros I, et al. Pressure-diameter relation of the human aorta. A new method of determination by the application of a special ultrasonic dimension catheter. *Circulation*. 1995;92:2210-9.
- Armentano RL, Graf S, Barra JG, Velikovsky G, Baglivo H, Sánchez R, et al. Carotid wall viscosity increase is related to intima media thickening in hypertensive patients. *Hypertension*. 1998;31:534-9.
- Gow BS, Taylor MG. Measurement of viscoelastic properties of arteries in the living dog. *Circ Res*. 1968;13:111-22.
- Armentano RL, Bia D, Craiem D, Gamero L, Levenson J, Grignola JC, et al. Respuesta en frecuencia de la pared arterial: ¿inocente o culpable de las discrepancias entre filtrado sistémico y pulmonar? *Rev Mex Ing Biom*. 2003;24:45-54.
- Wells SM, Langille BL, Adamson SL. In vivo and in vitro mechanical properties of the sheep thoracic aorta in the perinatal period and adulthood. *Am J Physiol Heart Circ Physiol*. 1998;274:H1749-H60.
- Bergel DH. The dynamic elastic properties of the arterial wall. *J Physiol London*. 1961;156:458-69.
- Bauer RD. Rheological approaches of arteries. *Biorheology*. 1984;1:159-67.
- Armentano RL, Barra JG, Levenson J, Simon A, Pichel RH. Arterial wall mechanics in conscious dogs. Assessment of viscous, inertial, and elastic moduli to characterize aortic wall behaviour. *Circ Res*. 1995;76:468-78.
- Guide for the Care and Use of Laboratory Animals. Institute for Laboratory Animal Research. National Research Council. Washington DC: National Academy Press; 1996.
- Fischer EI, Armentano RL, Pessana FM, Graf S, Romero L, Christen AI, et al. Endothelium-dependent arterial wall tone elasticity modulated by blood viscosity. *Am J Physiol Heart Circ Physiol*. 2002;282:H389-H94.
- Nichols WW, O'Rourke M. Mc Donald's blood flow in arteries: theoretical, experimental and clinical principles. 4th ed. London: Edward Arnold Publishers Ltd; 1998. p. 54-113; p. 201-22; p. 284-92, and p. 347-410.
- Shadwick RE. Mechanical design in arteries. *J Exp Biol*. 1999;202:3305-13.
- Fung YC. Biomechanics: mechanical properties of living tissues. 1st ed. New York-Heidelberg-Berlin: Springer Verlag; 1981. p. 34-6.
- Pontrelli G, Rossoni E. Numerical modelling of the pressure wave propagation in the arterial flow. *Int J Numer Meth Fluids*. 2003;43:651-71.
- Purslow PP. Positional variations in fracture toughness, stiffness and strength of descending thoracic pig aorta. *J Biomech*. 1983;16:947-53.
- Milnor WR. Hemodynamics. Baltimore: Williams & Wilkins; 1982. p. 56-96.
- Langewouters GJ, Wesseling KH, Goedhard WJ. The pressure dependent dynamic elasticity of 35 thoracic and 16 abdominal human aortas in vitro described by a five component model. *J Biomech*. 1985;18:613-20.
- Seifalian AM, Tiwari A, Hamilton G, Salacinski HJ. Improving the clinical patency of prosthetic vascular and coronary bypass grafts: the role of seeding and tissue engineering. *Artif Organs*. 2002;26:307-20.